Robust Fault Diagnosis of Hybrid Systems with Interval-Valued Uncertainties using Hybrid Bond Graph

Yacine Lounici,*[1,2] Youcef Touati,[1] Belkacem Ould Bouamama,[2] Smail Adjerid,[1] and Billal Nazim Chebouba[1,2]
[1]Solid Mechanics and Systems Laboratory (LMSS), Faculty of Technology, M'hmed Bougara University, Boumerdes 35000, Algeria.
[2]Centre de Recherche en Informatique, Signal et Automatique de Lille (CRISTAL), Polytech Lille, Université de Lille 1, France.
Email address: y.lounici@univ-boumerdes.dz/yacine.lounici@univ-lille.fr

***Abstract*—In this paper, a new robust fault diagnosis procedure for an uncertain hybrid system based on the hybrid bond graph model is proposed. The main objective is to enhance the robustness in the presence of uncertainties in order to minimize the non-detection and false alarm. The scientific interest of the present work remains in integrating the benefits of Hybrid bond graph and Interval analysis properties for effective diagnosis of uncertain hybrid systems. For this task, first, the Interval-valued Analytical redundancy relations which may undergo discrete mode changes are derived from diagnosis hybrid bond graph with controlled junctions. Secondly, the uncertainties are modelled directly in the hybrid bond graph as interval models for interval-valued thresholds generation. The limitations of the existing methods are alleviated by the proposed method. The effectiveness of the proposed method is demonstrated through simulation on a controlled two-tank hybrid system.**

Keywords—robust diagnosis; uncertain hybrid system; bond graph; interval-valued uncertainties; controlled junctions.

I. INTRODUCTION

Fault diagnosis for complex systems is a significant research area of modern industries in order to improve the reliability, safety and availability of systems. For this purpose, many fault diagnosis methods have been classified into signal-based and model-based. Details on these methods are presented in [1]. A recent review on fault diagnosis with hybrid/active and knowledge-based approaches is given in [2]. Most of the developed model-based methods are intended for systems that have a continuous behavioural evolution. However, large complex systems combine an exhibition of discrete and continuous modes and are hence called hybrid systems. The diagnosis of such systems gets complicated with the transition of modes from one to another.

In the last years, there have been considerable researches on the fault diagnosis of hybrid systems. For example, Heracleous and al. [3] proposed the use of a centralized fault diagnosis scheme for the detection and isolation of fault event in a hybrid system by considering the presence of parameter uncertainties. Zheng et al. [4], developed a new strategy based on the stochastic hybrid automata and unscented particle filter algorithm for the sensor faults diagnosis of the Lithium-ion battery hybrid system. An online fault diagnosis methodology with example scenarios generated from a hybrid hydraulic system is demonstrated in [5]. In this work, a global diagnosis model has been designed by integrating the observers and Timed Automata for detecting the faults and identifying the faulty component. In [6], the problem of the functional diagnosis of hybrid systems has been addressed for analytical redundancy construction. This problem was solved using the differential-algebraic, algebra of functions and pair algebra of partitions methods. However, most of the aforementioned works require many state-space equations to model complex hybrid systems which possess many modes and this imposes difficulty in fault diagnosis by making a comparison between state-space model and graphical model such as bipartite graphs, causal graphs and bond graph model [7]. Compared to the other graphical approaches the causal, structural and behavioural properties of the Bond Graph (BG) provides detailed information at the component level that allows the fault diagnosis to isolate the fault easily.

As BG model is based on the energy transfer phenomena to generate the analytical redundancy relation (ARR), there is considerable research on the robust diagnosis of continuous dynamic systems [8-10]. In recent works, the BG model has been extended to model not only for modeling but also for robust diagnosis and control of hybrid systems [11]. For instance, Ghoshal et al. [12] proposed the integration of the hybrid BG (HBG) and the approach for thresholds generation for systems having parameter uncertainties. Nevertheless, the thresholds are generated without taking into consideration the discrete mode changes. Another method based on the HBG linear fractional transformation (HBG-LFT) has been presented in [13], in order to generate the Global ARR (GARR) and thresholds for robust fault diagnosis of an uncertain hybrid system. In this context, Taktak et al. [14], developed a novel diagnosis algorithm HBG model and time-series data abstraction. However, all aforementioned works inherit one common drawback, that is, they consider the uncertain values with symmetric uncertainty limits over the nominal value. The unidirectional variation from the respective nominal value of certain values has not been taken into account.

The main contributions of this paper comparing with the cited and consulted works in the literature are listed as follows:

- The first contribution remains in integrating the benefits of HBG and Interval analysis (IA) properties leading to an efficient diagnosis of uncertain hybrid systems.
- Generation of new robust ARR to detect directly from the HBG in derivative causality. The robust ARR will be referred to as the Interval-valued GARR (I-GARR).
- Exploitation of the nominal part of I-GARR for residuals generation, while the uncertain part is used to generate the I-GARR thresholds. The latter leads to development of efficient thresholds that may enhance the robustness.

This paper is organized into five sections. In section 2, the proposed method based on HBG by considering the Interval-

978-1-7281-6999-6/20/$31.00 ©2020 IEEE

valued uncertainties is introduced. Also, the generation of the I-GARR and I-GARR thresholds for fault detection and isolation (FDI) are discussed therein. Section 3 presents the applicability of the proposed method by resorting to a controlled hybrid two-tank system. Section 4 shows the simulation results. In addition, a comparative study is made to assess the betterment in diagnosis performance. Finally, section 5 draws conclusions.

II. Fault Diagnosis using Interval-Valued Uncertainties in Hybrid Dynamic System

In HBG, the fault diagnosis is based on the generation of the GARR directly and systematically from the HBG-LFT model in preferred derivative causality using a covering causal path methodology. The GARR can be decoupled into two perfectly separable parts: nominal part and uncertain part. The nominal part of the GARR derived from the HBG-LFT model of the uncertain hybrid system is used for the generation of the residuals. The uncertain part of the GARR is used for adaptive thresholds generation over the nominal part. In general, the generated residuals are bounded between the equal lower threshold and upper threshold, because the uncertain values used for the calculation of the thresholds are considered with symmetric uncertainty limits over the respective nominal value. In other words, the deviation of the uncertainty on the left and the right sides over the nominal value is considered equal (symmetric over the nominal value of the parameter). However, certain uncertain values that vary in a unidirectional or asymmetric manner are not taken into consideration. Recently, Jha et al. [15] developed a new formalism of modeling the uncertainties in interval form using IA properties in BG approach for a diagnosis of continuous dynamics. This new formalism is adopted in this work to model the uncertainties in interval form for hybrid dynamic systems.

A. Interval-valued Uncertenties Modeling

The parameter uncertainties in hybrid systems can be represented in interval form on uncertain HBG model by decoupling the nominal value of the parameter $\theta_n = \{R_n, C_n, I_n, GY_n, TF_n\}$ from the uncertain part $\theta_n[\xi_n]$ where $\left[\underline{\xi_\theta}, \overline{\xi_\theta}\right] \cong [\xi_\theta]$. The uncertain parameter is modeled in interval form using the IA properties as shown in (1).

$$\left[\underline{\theta}, \overline{\theta}\right] = [\theta_n - \Delta\theta_l, \theta_n + \Delta\theta_r] \tag{1}$$

Where $\Delta\theta_l \geq 0$ and $\Delta\theta_r \geq 0$ are the additive deviation on the left and the right sides over the respective nominal value. The uncertain parameter θ can be represented in interval form as $\theta \in \left[\underline{\theta}, \overline{\theta}\right]$, in which $\theta \in \left[\underline{\theta}, \overline{\theta}\right] \Rightarrow \underline{\theta} \leq \theta \leq \overline{\theta}$. These properties can be exploited for any additive uncertainty modeling. The multiplicative uncertainty is defined as: $\xi_\theta = \Delta\theta / \theta_n$. The multiplicative uncertainty is expressed as,

$$\left[\underline{\xi_\theta}, \overline{\xi_\theta}\right] = [-\Delta\theta_l / \theta_n, +\Delta\theta_r / \theta_n] \tag{2}$$

Where $\xi_\theta \in \left[\underline{\xi_\theta}, \overline{\xi_\theta}\right]$.

The uncertain parameter θ can be expressed as,

$$\left[\underline{\theta}, \overline{\theta}\right] = \theta_n + \theta_n\left[\underline{\xi_\theta}, \overline{\xi_\theta}\right] \tag{3}$$

For more illustration, consider an uncertain resistance parameter R (e.g. electrical resistance, on/off control valve, mechanical damper, etc.) in resistance causality (imposed flow) as shown in Fig. 1.

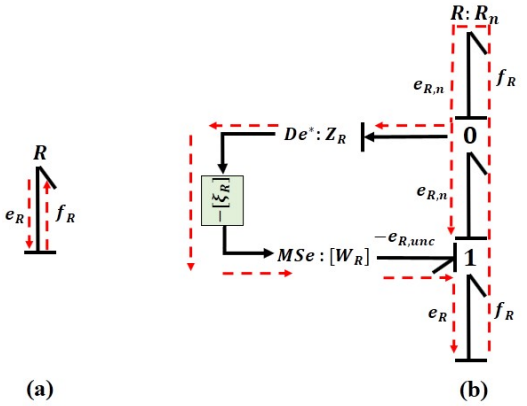

Fig. 1. (a) Nominal R element, (b) Uncertain R element in Interval form.

Where $MSe:[W_R]$ is the friction source (in this case effort source), and $De^*:Z_R$ is the virtual detector (in this case effort detector). In fact, the friction source is added to present the effort generated by the Interval-valued uncertainty. The virtual detector is added to present the information transfer. R_n is the nominal parameter value. $[\xi_R]$ is the parameter uncertainty in interval form. Finally, the characteristic equation of the two models are expressed as follows:

- Nominal case (see Fig. 1a): without any uncertainty

$$e_R = f_R.R \tag{4}$$

- Uncertain case (see Fig. 1b): with multiplicative interval uncertainty

$$\left[\underline{e_R}, \overline{e_R}\right] = f_R.\left(1 + \left[\underline{\xi_R}, \overline{\xi_R}\right]\right) \tag{5}$$

$$\left[\underline{e_R}, \overline{e_R}\right] = \underbrace{f_R.R_n}_{e_{R,n}} - \underbrace{[W_R]}_{-e_{R,unc}} \tag{6}$$

More definitions and properties of the IA analysis are detailed in [16].

B. Robust FDI using Interval-Valued Thresholds

Classically, a GARR is a constraint obtained from an observable and over-constrained hybrid system. For any function f is expressed in terms of known variables k. This function has the form: $f(k) = 0$.

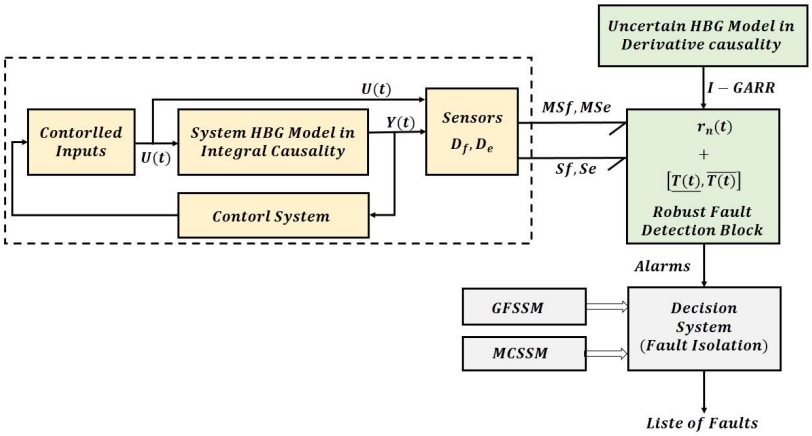

Fig. 2. Schematic description of the proposed fault diagnosis method in the presence of Interval-valued uncertainties.

In the HBG methodology, an $GARR: f(U,Y,\theta,a_{bj})=0$, where, U represents the input vector $(SSf(t), SSe(t))$, Y represents the known vector of sensor output $(Sf(t), Se(t))$ and θ_n represents the parameters system vector. a_{bj} represents the vector of the controlled junction mode, $a_{bj}=[a_{b1}, a_{b2}, ..., a_{bm}]$, where $a_{bj}\in\{0,1\}$ for $j=1,...,m$ with m is the number of the controlled junctions (Table. 1). For the uncertain HBG systems, robust FDI is achieved by generation of uncertain GARR with two separable parts: uncertain part and nominal part. This approach is extended in this paper to obtain the I-GARR in the presence of Interval-valued uncertainties, as described in Fig. 2.

The I-GARR can be obtained by the following rules (Fig. 2):

Step1: Put the nominal HBG model in derivative causality, then model the Interval-valued uncertainties as explained previously to obtain the uncertain HBG model.

Step2: Calculate the candidate I-GARR from the "0" or "1" junctions.

Step3: The known variables are eliminated using dualized detectors to obtain the I-GARR consisting of the nominal and uncertain parts. The nominal part is used for residuals $r_n(t)$ generation as shown in (7). The interval-valued uncertainty part is perfectly separated from the nominal part to obtain the interval-valued Thresholds $\left[\underline{T(t)}, \overline{T(t)}\right]$ (8). The two functions is characterized by point valued function Φ_i.

$$r_n(t)=\Phi_1\left(Sf, Se, SSf(t), SSe(t), \theta_n\right) \tag{7}$$

$$\left[\underline{T(t)}, \overline{T(t)}\right]=\Phi_2\left(\left[\underline{\xi_\theta}, \overline{\xi_\theta}\right], SSf(t), SSe(t), \left[\underline{\theta}, \overline{\theta}\right]\right) \tag{8}$$

Finally, $r_n(t)$ will be termed nominal residuals (numerical evaluation of the point-valued function Φ_1 and Φ_2 will be referred to as Interval-valued thresholds function.

The robust fault detection algorithm using the Interval-valued thresholds proposed in this is given in Table. 1.

TABLE I. PROPOSED ROBUST FAULT DETECTION ALGORITHM

$$\textbf{\textit{Input}}: \left\{\begin{array}{l}\Phi_1^i\left(Sf, Se, SSf(k), SSe(k), \theta_n, a_{bj}\right)\\ \Phi_2^i\left(\left[\underline{\xi_\theta}, \overline{\xi_\theta}\right], SSf(k), SSe(k), \left[\underline{\theta}, \overline{\theta}\right], a_{bj}\right)\end{array}\right\}$$

Output : *Robust fault detection*

$$r_n(t)=\Phi_1\left(Sf, Se, SSf(k), SSe(k), \theta_n, a_{bj}\right)$$

$$\left[\underline{T(k)}, \overline{T(k)}\right]=\Phi_2\left(\left[\underline{\xi_\theta}, \overline{\xi_\theta}\right], SSf(k), SSe(k), \left[\underline{\theta}, \overline{\theta}\right], a_{bj}\right)$$

If $-r_n(k)\le\overline{T(k)}$ *and* $-r_n(k)\ge\underline{T(k)}$

faults detection ← ***false***

else

faults detection ← ***true***

end If

Once all I-GARR are obtained by the proposed method, the faults that can be isolated must be concluded. As we know Hybrid dynamical systems contain both discrete and continuous modes. So, the fault isolation step is needed to be separately derived for each mode. So, in this work, we use two essential definitions the Global Fault Sensitivity Signature Matrix (GFSSM) and Mode Change Sensitivity Signature Matrix (MCSSM) [17]. The GFSSM is able (1) to differentiate between the decreasing $(P_j\downarrow)$ and increasing $(P_j\uparrow)$ and (2) to differentiate between the faults signatures. The MCSSM is able to differentiate between mode fault decreasing $(a_k\downarrow)$ and increasing $(a_k\uparrow)$.

III. APPLICATION

The aim of this section is to give practical insights about the applicability and performance of the proposed method. The application is carried out a controlled two-tank hybrid system, which is adopted from [12]. The schematic of this system is shown in Fig. 3.

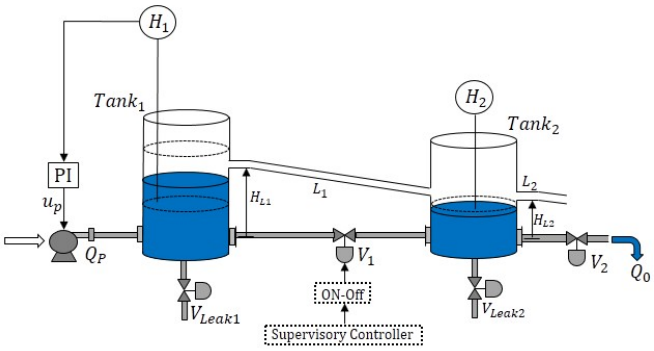

Fig. 3. Shematic of a controlled two-tank hybrid system.

This system contains two tanks (Tanks$_i$, $i=1,2$) which is connected with two non-linear valves (V_1 and V_2) whose coefficients of discharge are C_{dV1} and C_{dV2} respectively. Tank T_1 is equipped with a hydraulic pump which is controlled by a Proportional-Integral (PI) controller to maintain the liquid level of 0.5m. The controlled flow delivered by the pump Q_P to the Tank T_1 is proportional to the PI-controller output. The Tank T_1 is equipped with a drainage pipe (L_1) to drain the liquid toward Tank T_2 when $H_1(t) > H_{L1}$ (autonomous mode, a_1). Similarly, Tank T_2 drains out liquid through a drainage pipe (L_2) when $H_2(t) > H_{L2}$ (autonomous mode, a_2). These drainage pipes show linear behavior with coefficients of discharge (C_{dL1} and C_{dL2}). Each of Tanks has an imaginary valve with coefficients of discharge $C_{Leaki}, i=1,2$. The system hybrid dynamics includes supervisory and autonomous controller transition modes. The measurements architecture of this system is composed of a flow sensor for liquid input pump measurement and two-level sensors (H_1 and H_2) for measuring levels in T_1 and T_2.

The uncertain HBG model of the controlled two-tank hybrid system in derivative causality is shown in Fig. 4. After representing the Interval-valued uncertainties in the uncertain HBG model, in which all storage elements and the two controlled junctions are assigned with appropriate causality the obtained ARR and I-GARR are listed as follows:

$$ARR_1 : Q_p - \Psi(U_{PI}) = 0 \tag{9}$$

$$ARR_2 : U_{PI} - \Psi_{PI} = 0 \tag{10}$$

Not that the obtained ARRs represent the actuator and the PI-controller, and do not contain code change parameters.

$$\begin{aligned}&\left[\underline{I-GARR_3}, \overline{I-GARR_3}\right] : Q_p - a_1.C_{dL1}.\rho.g.\left(H_1(t)-H_{L1}(t)\right)\\ &-a_{V1}.C_{dV1}.\sqrt{\left|\rho.g.\left(H_1(t)-H_2(t)\right)\right|}.sign\left(\rho.g.\left(H_1(t)-H_2(t)\right)\right)\\ &-C_{T1}\frac{d}{dt}\left(\rho.g.H_1(t)\right) - C_{Leak1}.\sqrt{\left|\rho.g.H_1(t)\right|} + \left[\underline{T_3(t)}, \overline{T_3(t)}\right] = 0\end{aligned} \tag{11}$$

$$\begin{aligned}&\left[\underline{I-GARR_4}, \overline{I-GARR_4}\right] : a_1.C_{dL1}.\rho.g.\left(H_1(t)-H_{L1}(t)\right)\\ &-a_{V1}.C_{dV1}.\sqrt{\left|\rho.g.\left(H_1(t)-H_2(t)\right)\right|}.sign\left(\rho.g.\left(H_1(t)-H_2(t)\right)\right)\\ &-a_2.C_{dL2}.\rho.g.\left(H_2(t)-H_{L2}(t)\right) - C_{dV2}.\sqrt{\left|\rho.g.H_2(t)\right|}\\ &-C_{Leak22}.\sqrt{\left|\rho.g.H_2(t)\right|} - C_{T1}\frac{d}{dt}\left(\rho.g.H_1(t)\right) + \left[\underline{T_4(t)}, \overline{T_4(t)}\right] = 0\end{aligned} \tag{12}$$

Where the I-GARR are expressed as,

$$\left[\underline{I-GARR_3}, \overline{I-GARR_3}\right] : r_{3,n} + \left[\underline{T_3(t)}, \overline{T_3(t)}\right] \tag{13}$$

$$\left[\underline{I-GARR_4}, \overline{I-GARR_4}\right] : r_{4,n} + \left[\underline{T_4(t)}, \overline{T_4(t)}\right] \tag{14}$$

Note that $r_{3,n}$ and $r_{4,n}$ are the numerical evaluation (residuals) of the nominal part of $I-GARR_3$ and $I-GARR_4$ respectively. Hence the adaptive thresholds calculated using the Interval-valued uncertainties are obtained in (15) and (16).

$$\begin{aligned}\left[\underline{T_3(t)}, \overline{T_3(t)}\right] &= \left|\left[\underline{\xi_{C_{dL1}}}, \overline{\xi_{C_{dL1}}}\right].a_1.C_{dL1}.\rho.g.\left(H_1(t)-H_{L1}(t)\right)\right|\\ &+\left|\left[\underline{\xi_{C_{dV1}}}, \overline{\xi_{C_{dV1}}}\right].a_{V1}.C_{dV1}.\sqrt{\left|\rho.g.\left(H_1(t)-H_2(t)\right)\right|}\right|\\ &+\left|\left[\underline{\xi_{C_{T1}}}, \overline{\xi_{C_{T1}}}\right].C_{T1}\frac{d}{dt}\left(\rho.g.H_1(t)\right)\right| + \left|\left[\underline{\xi_{C_{Leak1}}}, \overline{\xi_{C_{Leak1}}}\right].C_{Leak1}.\sqrt{\left|\rho.g.H_1(t)\right|}\right|\end{aligned} \tag{15}$$

$$\begin{aligned}\left[\underline{T_4(t)}, \overline{T_4(t)}\right] &= \left|\left[\underline{\xi_{C_{dL1}}}, \overline{\xi_{C_{dL1}}}\right].a_1.C_{dL1}.\rho.g.\left(H_1(t)-H_{L1}(t)\right)\right|\\ &+\left|\left[\underline{\xi_{C_{dV1}}}, \overline{\xi_{C_{dV1}}}\right].a_{V1}.C_{dV1}.\sqrt{\left|\rho.g.\left(H_1(t)-H_2(t)\right)\right|}\right|\\ &+\left|\left[\underline{\xi_{C_{dL2}}}, \overline{\xi_{C_{dL2}}}\right]a_2.C_{dL2}.\rho.g.\left(H_2(t)-H_{L2}(t)\right)\right| + \left|\left[\underline{\xi_{C_{dV2}}}, \overline{\xi_{C_{dV2}}}\right]C_{dV2}.\sqrt{\left|\rho.g.H_2(t)\right|}\right|\\ &+\left|\left[\underline{\xi_{C_{Leak2}}}, \overline{\xi_{C_{Leak2}}}\right]C_{Leak2}.\sqrt{\left|\rho.g.H_2(t)\right|}\right| + \left|\left[\underline{\xi_{C_{T1}}}, \overline{\xi_{C_{T1}}}\right]C_{T1}\frac{d}{dt}\left(\rho.g.H_1(t)\right)\right|\end{aligned} \tag{16}$$

Using the I-GARR, the MCSSM and GFSSM for the controlled two-tank hybrid system are deduced as shown in Table. 1 and Table. 2, respectively.

TABLE 1. MCSSM FOR THE TWO-TANK HYBRID SYSTEM

Parameter	$I-GARR_3(r_3)$	$I-GARR_4(r_4)$	M_f	I_f
$a_{V1}\uparrow$	1	−1	1	1
$a_{V1}\downarrow$	−1	1	1	1

IV. SIMULATION RESULTS

This section illustrates and compares the obtained results with an existing method (HBG-LFT model-based fault diagnosis). No-fault is introduced to the controlled two-tank hybrid system in the first scenario. The input and output variables of the system are shown in Fig. 5.

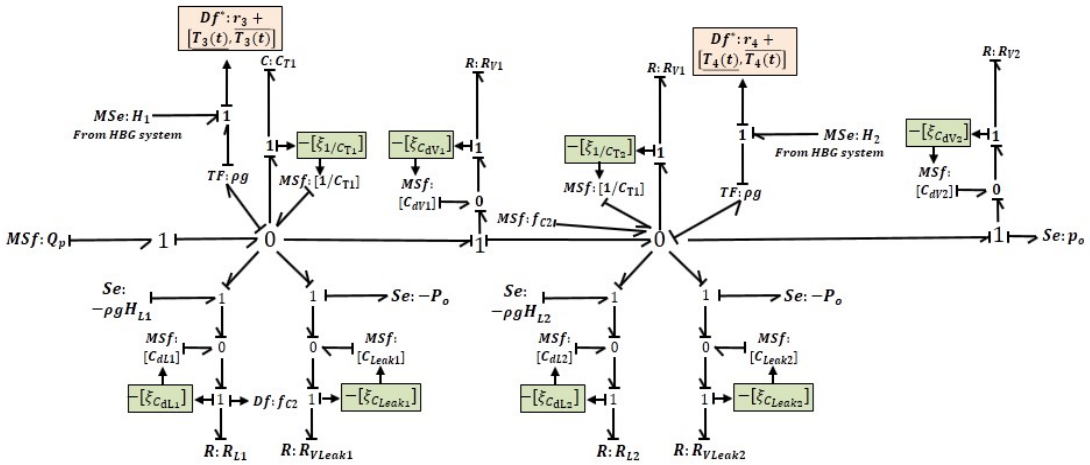

Fig. 4. HBG model in the presence of Interval-valued uncertainties (derivative causality for robust diagnosis purposes).

TABLE 2. GFSSM FOR THE TWO-TANK HYBRID SYSTEM

Parameter	r_3	r_4	M_f	I_f
$C_{dV1}\uparrow$	a_{V1}	$-a_{V1}$	a_{V1}	$\overline{a_{V1}}=(1-a_1)a_{V1}$
$C_{dV1}\downarrow$	$-a_{V1}$	a_{V1}	a_{V1}	$\overline{a_{V1}}=(1-a_1)a_{V1}$
$C_{dL1}\uparrow$	a_1	$-a_1$	a_1	$\overline{a_1}=(1-a_{V1})a_1$
$C_{dL1}\downarrow$	$-a_1$	a_1	a_1	$\overline{a_1}=(1-a_{V1})a_1$
$C_{dL2}\uparrow$	0	a_2	a_2	0
$C_{dL2}\downarrow$	0	$-a_2$	a_2	0
$C_{dV2}\uparrow$	0	+1	1	0
$C_{dV2}\downarrow$	0	−1	1	$\overline{a_{V1}}=(1-a_2)$

The residuals (r_3 and r_4) and their lower thresholds $\underline{T_3(t)}$ and $\underline{T_4(t)}$, (red dashed lines) and upper thresholds $\overline{T_3(t)}$ and $\overline{T_4(t)}$ (green dashed lines) are obtained from the uncertain HBG model (Fig. 4) as depicted in Fig. 6. We remark that the two residuals are close to zero and do not exceed the Interval-valued thresholds. Hence, a healthy situation is identified correctly by the proposed method. Not that the uncertain values are presented in Table. 3.

TABLE 3. INTERVAL-VALUED UNCERTAINTIES VALUES

Parameter (Nominal Value)	Uncertainty Value
$C_{dVi}=1.59\times10^{-2}\,kg^{1/2}m^{1/2}$	$\left[\underline{\xi_{C_{dVi}}},\overline{\xi_{C_{dVi}}}\right]=\left[0,0.745\times10^{-3}\right]$
$C_{dLi}=1\times10^{-3}\,ms$	$\left[\underline{\xi_{C_{dLi}}},\overline{\xi_{C_{dLi}}}\right]=\left[-0.43\times10^{-4},0.81\times10^{-4}\right]$
$C_{Ti}=1.5\times10^{-3}\,ms^2$	$\left[\underline{\xi_{C_{Ti}}},\overline{\xi_{C_{Ti}}}\right]=\left[-0.0015,0.008\right]$
$C_{dLeaki}=0kg^{1/2}m^{1/2}$	$\left[\underline{\xi_{C_{dLeaki}}},\overline{\xi_{C_{dLeaki}}}\right]=\left[0,0.12\times10^{-4}\right]$

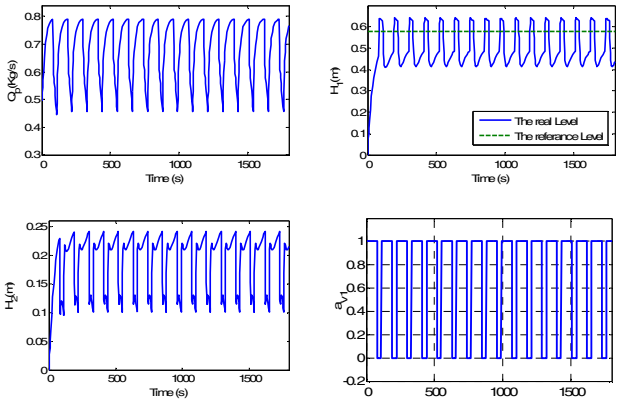

Fig. 5. The input and outputs of the controlled two-tank hybrid system.

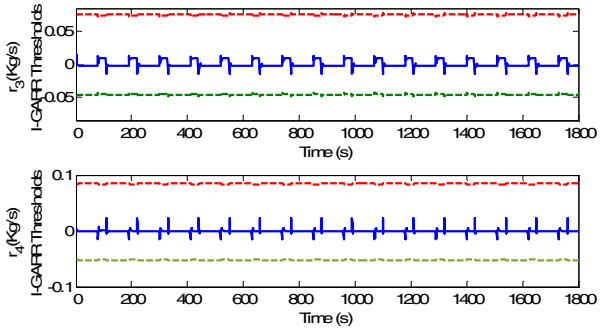

Fig. 6. Residuals and thresholds in normal functioning.

Leakage fault in Valve V1 ($C_{dV1}\uparrow$) : a fault is introduced on the valve (V_1) $(1.3C_{dV1})$ at time t=800s. As shown in Fig. 7, r_3 and r_4 deviate outside the upper threshold and the lower threshold respectively. In addition, the signature $\{a_{v1},-a_{v1}\}$ is the same as the signature of $(C_{dV1}\uparrow)$ (Table. 2). Finally, it possible to conclude that the faulty valve is detected and isolated correctly by the proposed method. Not that this fault is detected until the system moves into $\{a_{v1}=1\}$.

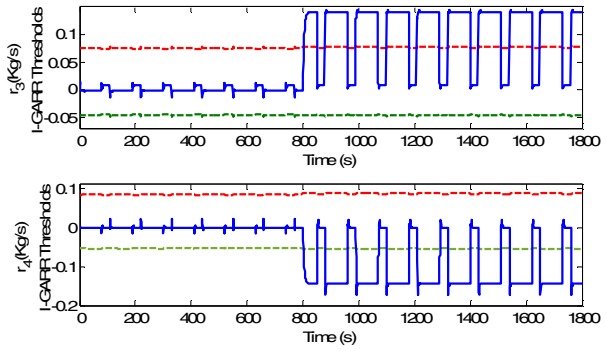

Fig. 7. Residuals and thresholds in the case of leakage fault in Valve V_1.

Blockage fault in Valve V_2 ($C_{dV2} \downarrow$): This fault ($0.7C_{dV2}$) is introduced at t=1000s. As observed in Fig.8, r_4 deviates outside the upper threshold. r_3 does not detect this fault because it is not sensitive to it. The HBG-LFT thresholds are symmetric in nature. Moreover, the width of the thresholds is greater in magnitude than the thresholds generated by the proposed method. The introduced fault is detected and isolated $\{0,-1\}$ (see Table. 2) correctly by the proposed method. On the contrary, HBG-LFT method produces over-estimated thresholds that lead to non-detection of the blockage fault on the valve (V_2) as shown in Fig. 8.

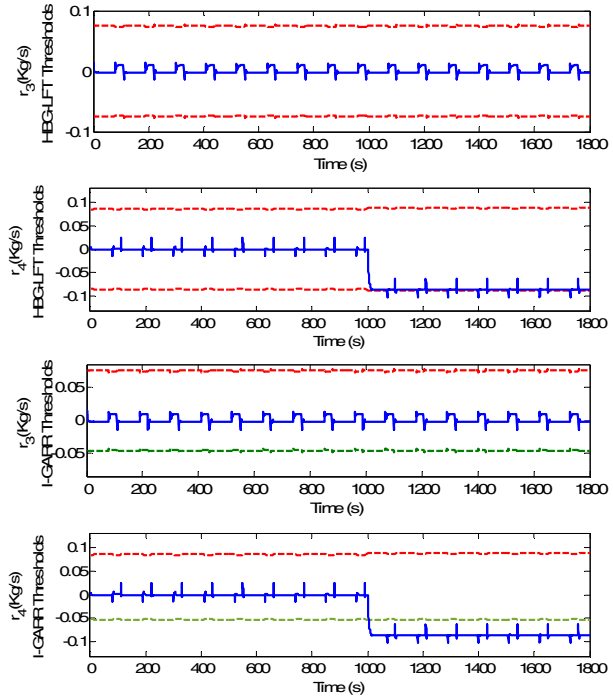

Fig. 8. Residuals and thresholds generation using the HBG-LFT method [12-14], and the proposed method in the case of blockage fault in Valve V_2.

V. CONCLUSIONS

It has been successfully demonstrated that the proposed method can be used for the development of the robust fault diagnosis. By the generation of the I-GARR and interval-valued thresholds alleviate the limitations associated with the HBG-LFT methods. Moreover, it has been shown that the proposed method is successful in generating optimal thresholds. The simulation studies have demonstrated the performance of the I-GARR based robust fault diagnosis.

REFERENCES

[1] Z. Gao, SX, Ding and C. Cecati "A surve-y of fault diagnosis and fault-tolerant techniques—Part I: Fault diagnosis with model-based and signal-based approaches," IEEE Transactions on Industrial Electronics, vol. 62, no 6, pp. 3757-3767, 2015.

[2] Z. Gao, C. Cecati, and S. X. Ding, "A Survey of fault diagnosis and fault-tolerant techniques—Part II: Fault diagnosis with knowledge-based and hybrid/active approaches," IEEE Trans. Ind. Electron., vol. 62, no. 6, pp. 3768–3774, Jun. 2015.

[3] C. Heracleous, C. G. Panayiotou and M. M. Polycarpou, "Fault Diagnosis of Uncertain Hybrid Systems," IFAC-Papers OnLine, vol. 51, no 24, pp. 123-130, 2018.

[4] C. Zheng, Z. Chen and D. Huang, "Fault diagnosis of voltage sensor and current sensor for lithium-ion battery pack using hybrid system modeling and unscented particle filter," Energy, vol. 191, pp. 116504, 2020.

[5] L. Mhamdi, B. Maaref, H. Dhouibi, H. Messaoud and Z. S. Abazi, "Diagnosis of hybrid systems through observers and timed automata," In 2016 International Conference on Control, Decision and Information Technologies (CoDIT) IEEE, pp. 164-169, April. 2016.

[6] A. N. Zhirabok and A. E.Shumsky, " Redundancy Relations for the Diagnosis of Hybrid Systems" Journal of Computer and Systems Sciences International, vol. 57, no 4, p. 594-607, March. 2018.

[7] F. Yang, P. Duan, S. L. Shah and T. Chen, "Capturing connectivity and causality in complex industrial processes," Springer Science and Business Media, 2014.

[8] Y. Touati, R. Merzouki and B. O. Bouamama, " Robust diagnosis to measurement uncertainties using bond graph approach: Application to intelligent autonomous vehicle," Mechatronics, vol. 22, no 8, pp. 1148-1160, 2012.

[9] Y. Lounici, Y. Touati and S. Adjerid, "A Comparison of Bond Graph Model-Based Methods for Fault Diagnosis in the Presence of Uncertainties: Application to Mechatronic System," In 2019 International Conference on Advanced Electrical Engineering (ICAEE) IEEE, pp. 1-8, November. 2019.

[10] Y. Lounici, Y. Touati and S. Adjerid, "Uncertain fault estimation using bicausal bond graph: Application to intelligent autonomous vehicle," Proceedings of the Institution of Mechanical Engineers, Part I: Journal of Systems and Control Engineering, 0959651819892379, December. 2019.

[11] W. Borutzky, "Bond graph model-based fault diagnosis of hybrid systems" Switzerland: Springer International Publishing, 2015.

[12] S. K. Ghoshal, S. Samanta and A. K. Samantaray, "Robust fault detection and isolation of hybrid systems with uncertain parameters," Proceedings of the Institution of Mechanical Engineers, Part I: Journal of Systems and Control Engineering, vol. 226, no 8, pp. 1013-1028, 2012.

[13] M. I. Rahal, B. O. Bouamama and A. Meghebbar, "Hybrid bond graph for robust diagnosis to measurement uncertainties," In 2016 5th International Conference on Systems and Control (ICSC) IEEE, p. 439-444, May. 2016.

[14] M. Taktak, S. Triki, and A. Kamoun, "Real time algorithm based on time series data abstraction and hybrid bond graph model for diagnosis of switched system," Engineering Applications of Artificial Intelligence, vol. 59, pp. 51-72, 2017.

[15] M. S. Jha, G. Dauphin-Tanguy and B. Ould-Bouamama, "Robust fault detection with interval valued uncertainties in bond graph framework," Control Engineering Practice, vol. 71, p. 61-78, 2018.

[16] R. E. Moore, R. B. Kearfott and M. J. Cloud, "Introduction to interval analysis," Siam. Vol. 110, 2009.

[17] R. Levy, S. Arogeti, D. Wang and O. Fivel, "Improved diagnosis of hybrid systems using instantaneous sensitivity matrices," Mechanism and Machine Theory, vol. 91, pp. 240-257, 2015.